J Physiol 593.5 (2015) pp 1273–1289

The Journal of Physiology

Essential amino acid transporter Lat4 (*Slc43a2*) is required for mouse development

Adriano Guetg[1], Luca Mariotta[1], Lukas Bock[1], Brigitte Herzog[1], Ralph Fingerhut[2], Simone M. R. Camargo[1] and François Verrey[1]

[1] *Institute of Physiology and Zurich Center of Integrative Human Physiology, University of Zurich, Switzerland*
[2] *University Children's Hospital, Children's Research Center, Zurich, Switzerland*

Key points

- Lat4 (*Slc43a2*) transports branched-chain amino acids, phenylalanine and methionine, and is expressed in kidney tubule and small intestine epithelial cells.
- Using a new knockout model as a negative control, it is shown that Lat4 is expressed at the basolateral side of small intestine enterocytes and kidney epithelial cells of the proximal tubule, thick ascending limb and distal convoluted tubule.
- In the *Xenopus* oocyte expression system, Lat4 is shown to function as a uniporter with symmetric intracellular and extracellular apparent affinities for phenylalanine.
- Mice lacking Lat4 display a slight intrauterine growth restriction, postnatal malnutrition and early death, presumably as a result of defective amino acid (re)absorption.
- These results demonstrate the crucial role that the uniporter Lat4 plays for amino acid transport across cellular barriers and mouse development.

Abstract Amino acid (AA) uniporter Lat4 (*Slc43a2*) mediates facilitated diffusion of branched-chain AAs, methionine and phenylalanine, although its physiological role and sub-cellular localization are not known. We report that *Slc43a2* knockout mice were born at expected Mendelian frequency but displayed an ∼10% intrauterine growth retardation and low amniotic fluid AAs, suggesting defective transplacental transport. Postnatal growth was strongly reduced, with premature death occurring within 9 days such that further investigations were made within 3 days of birth. Lat4 immunofluorescence showed a strong basolateral signal in the small intestine, kidney proximal tubule and thick ascending limb epithelial cells of wild-type but not *Slc43a2* null littermates and no signal in liver and skeletal muscle. Experiments using *Xenopus laevis* oocytes demonstrated that Lat4 functioned as a symmetrical low affinity uniporter with a $K_{0.5}$ of ∼5 mM for both in- and efflux. Plasma AA concentration was decreased in *Slc43a2* null pups, in particular that of non-essential AAs alanine, serine, histidine and proline. Together with an increased level of plasma long chain acylcarnitines and a strong alteration of liver gene expression, this indicates malnutrition. Attempts to rescue pups by decreasing the litter size or by nutrients injected I.P. did not succeed. Radioactively labelled leucine but not lysine given *per os* accumulated in the small intestine of *Slc43a2*null pups, suggesting the defective transcellular transport of Lat4 substrates. In summary, Lat4 is a symmetrical uniporter for neutral essential AAs localizing at the basolateral side of (re)absorbing epithelia and is necessary for early nutrition and development.

(Resubmitted 5 September 2014; accepted after revision 25 November 2014; first published online 4 December 2014)
Corresponding author F. Verrey: Institute of Physiology, University of Zürich, Winterthurerstrasse 190, CH-8057 Zürich, Switzerland. Email: verrey@access.uzh.ch

Abbreviations AA, amino acid; DA, dicarboxylacylcarnitine; E, embryonic day; KO, knockout; NCC, sodium-chloride cotransporter; NKCC2, sodium-potassium-chloride cotransporter 2; RT, room temperature.

DOI: 10.1113/jphysiol.2014.283960

Introduction

Dietary protein intake is an essential and tightly regulated process that needs to meet physiological body requirements, especially during highly anabolic periods (Poncet & Taylor, 2013). The enzyme-mediated hydrolysis of dietary proteins in the gastrointestinal lumen produces oligopeptides and individual amino acids (AAs) that are absorbed by moving sequentially across apical and basolateral cell membranes of small intestine enterocytes (Nassl *et al.* 2011). The zwitterionic nature of neutral AAs prevents the direct crossing of the epithelial lipid bilayer by simple diffusion and imposes the presence of membrane-spanning transporter proteins (Braun *et al.* 2011). Severe malabsorption and aminoaciduria syndromes have been linked to defects of specific AA transporters, substantiating the essential role that transepithelial transport plays for body AA homeostasis (Verrey *et al.* 2009; Broer & Palacin, 2011).

The luminal step of neutral AA absorption and reabsorption at the level of the small intestine and kidney, respectively, is largely mediated by the apical transporter B^0AT1 (*SLC6A19*). This luminal symporter uses the driving force exerted by the Na^+ gradient and the membrane potential on the co-transported Na^+ ion for the concentrative import of its neutral AA substrates (secondary active transport) (Rudnick *et al.* 2014). Once inside enterocytes or kidney proximal tubule cells, neutral AAs can be effluxed across the basolateral membrane by cooperating AA exchangers and uniporters. Indeed, all neutral AAs can be effluxed by the major basolateral neutral AA anti-porter (obligatory exchanger) LAT2–4F2hc (*SLC7A8-SLC3A2*). It is, however, important to realize that, for each exported AA, this anti-porter imports another AA. Thus, this anti-porter does not perform a net transmembrane AA efflux (Meier *et al.* 2002). Unexpectedly, no genetic diseases involving defects of LAT2–4F2hc have been described to date, whereas mutations in the other basolateral anti-porter y^+LAT1–4F2hc (*SLC7A7-SLC3A2*), which exchanges preferentially intracellular cationic AAs against neutral AAs and Na^+, cause lysinuric protein intolerance, an autosomal recessive disease (Borsani *et al.* 1999). The respective physiological roles of both exchangers were also investigated using knockout (KO) mice. The lack of LAT2 resulted in a mild phenotype with a minor aminoaciduria (Braun *et al.* 2011), whereas the lack of y^+LAT1 caused intrauterine growth restriction and resulted in premature death for ∼90% of newborn *Slc7a7*$^{-/-}$ homozygous mice (Sperandeo *et al.* 2007).

To achieve a net efflux of all different AAs from small intestine enterocytes and proximal kidney tubule epithelial cells, transporters are required to mediate the net efflux of some AAs that can then recycle into the cells via the above mentioned anti-porters and thereby drive their efflux activity (Verrey *et al.* 2009). The T-type aromatic AA uniporter TAT1 (*SLC16A10*) represents the best characterized such transporter expressed at the basolateral membrane (Ramadan *et al.* 2006; Ramadan *et al.* 2007). Using the *Xenopus laevis* oocyte expression system, it was shown to mediate facilitated diffusion of the essential aromatic AAs phenylalanine, tryptophan and tyrosine with symmetric apparent affinities (i.e. $K_m \approx 30$ mM for phenylalanine) and thereby drive the efflux of other LAT2–4F2hc substrates such as the non-essential AA glutamine (Ramadan *et al.* 2006; Ramadan *et al.* 2007). Recently, we characterized the physiological role of TAT1 using *Slc16a10* deficient mice. Interestingly, these mice presented a mild phenotype with increased plasma, kidney and muscle aromatic AAs, independently of dietary protein quantity, combined with a major aromatic aminoaciduria under a high protein diet (Mariotta *et al.* 2012). The lack of neurological symptoms and important metabolic dysfunctions, despite the defective intestinal absorption of aromatic AAs such as tyrosine, which is the metabolic precursors of the hormone thyroxine and the neurotransmitter dopamine, suggested a possible compensatory mechanism by (an)other basolateral uniporter(s). We proposed that the uniporter LAT4 (*SLC43A2*) could play this role.

LAT4 belongs to the SLC43 family that includes two additional members: LAT3 (*SLC43A1*), which is a uniporter for large essential neutral AAs and has been shown to be upregulated in liver and skeletal muscle upon starvation and displays only a low mRNA expression level in the small intestine and kidney (Babu *et al.* 2003; Fukuhara *et al.* 2007), and EEG1 (*SLC43A3*), the function of which remains unknown. The latter gene product was shown to be prominently expressed in human liver and heart and, based on immunohistochemistry, to be expressed at the basolateral membrane of human kidney proximal convoluted tubule (Bodoy *et al.* 2005). LAT4 shows only ∼30% identity with EEG1 and has been shown by Northern blot analysis of human RNA to be highly expressed in placenta, peripheral blood leucocytes and kidney and, additionally, by Northern blot analysis of mouse RNA, to be expressed in the small intestine and brain (Bodoy *et al.* 2005). Microarray data (www.biogps.org) confirm this expression pattern and additionally show substantial expression in macrophages, microglia and osteoclasts. Based on *in situ* hybridization, Lat4 was suggested to be expressed in the kidney distal tubule and collecting duct and the images also appeared to be compatible with expression in the proximal tubule. In the small intestine, the signal was localized more to crypt cells (Bodoy *et al.* 2005). Lat4 mRNA was also detected in cell lines isolated from the mouse kidney proximal tubule, in agreement with the mRNA expression in isolated proximal tubules reported by Cheval *et al.* (2011). Furthermore, kinetic analysis of phenylalanine uptake in

these cells suggested the involvement of Lat4, supporting the possibility that this uniporter plays a role in proximal tubule AA reabsorption.

The preferential substrates of LAT4 comprise only essential AAs, specifically the branched-chain ones (leucine, isoleucine, valine) and additionally phenylalanine and methionine (Bodoy *et al.* 2005). To test the physiological role of Lat4 in whole-body AA homeostasis and epithelial transport, we generated a global *Slc43a2*$^{-/-}$ KO mouse and we now report the analysis of its phenotype.

Methods

Ethical approval

All procedures for mice and *X. laevis* frogs handling and experimental interventions were performed in accordance with Swiss Animal Welfare laws and approved by the Cantonal Veterinary Office, Zürich.

Generation of *Slc43a2*/*Lat4*$^{-/-}$ KO mice by gene trapping

The *Slc43a2*$^{-/-}$ KO mouse was produced by the Phenogenomic Center of Toronto (www.phenogenomics.ca). Embryonic stem cell lines were mutated by insertional mutagenesis using a UPA gene trap vector (Shigeoka *et al.* 2005) in the sixth intron of the *Slc43a2* gene. Cells were prepared for aggregation with diploid embryos to produce chimeric mice. R1 cells were on a 129 mouse background, whereas the germline was tested by crossing the chimera to CD-1 mice and assessing coat colour. The interruption of the gene leads to the production of a truncated transcript presumably subject to nonsense-mediated decay and thus of low abundance. Mice were bred on a C57BL/6 background. All animals were housed under standard conditions and fed a standard diet prior to experimentation.

Antibodies

Anti-mouse Lat4 antibodies targeted to the C-terminal peptide (N-CQLQQKREDSKLFL-C) were raised in rabbit, whereas anti-mouse Tmem27 antibodies targeted to the C-terminal peptide (N-CDPLDMKGGHINDGFLT-C) and anti-mouse B^{0}AT1 antibodies targeted to the N-terminal peptide (N-MVRLVLPNPGLEERIC-C) were raised in guinea-pig (Pineda, Berlin, Germany). Anti-mouse sodium-chloride cotransporter (NCC) (Loffing *et al.* 2004), anti-mouse sodium-potassium-chloride cotransporter 2 (NKCC2) (Kaplan *et al.* 1996) and anti-mouse MDR1 (Fickert *et al.* 2001) were previously characterized. For β-actin detection, a commercially available mouse anti-β-actin antibody was used (Sigma-Aldrich, Buchs, Switzerland).

Immunofluorescence

Organs were isolated and immediately frozen in liquid propane. Sections, 7 μm thick, were prepared on Superfrost Plus Menzel slides (Gerhard Menzel GmbH, Braunschweig, Germany). To test for Lat4 localization in NKCC2 expressing kidney tubule segments, 4 μm consecutive sections were prepared. Sections were then fixed with methanol at −20°C for 90 s, rehydrated for 15 min at room temperature (RT) and washed three times for 5 min with PBS at RT. For Lat4, NCC, MDR1, Tmem27 and B°AT1 detection, epitope retrieval was performed by incubating slides in 10 mM sodium citrate (pH 6.0) for 10 min at 98°C with a microwave (Histos 3; Milestone, Shelton, CT, USA). For NKCC2 and Tat1 detection, no epitope retrieval was performed. Sections were then washed again three times for 5 min with PBS at RT and incubated with blocking solution (2% BSA, 0.04% Triton X-100 in PBS, pH 7.4) for 1 h at RT. Primary antibodies were diluted in blocking solution and incubated overnight at 4°C with the respective dilutions: 1:500 for Lat4, 1:1000 for Tmem27, 1:2000 for NKCC2, 1:500 for NCC, 1:500 for Tat1, 1:300 for MDR1 and 1:500 for B°AT1. Sections were then washed three times for 5 min in PBS at RT. Secondary antibodies were applied at 1:500 dilutions for 1 h at RT: Alexa Fluor 488 anti-rabbit, Alexa Fluor 594 anti-rabbit and Alexa Fluor 568 anti-guinea-pig (Molecular Probes, Life Technologies, Grand Island, NY, USA). Staining of nuclei was performed with 4′,6-diamidino-2-phenylindole at 1:500 dilution.

Western blotting on oocyte total membrane lysates

Total membrane lysates of oocytes and western blotting were performed as described previously (Ramadan *et al.* 2007). For β-actin detection, the antibody was applied at 1:5000 dilution. For Lat4 detection, the antibody was applied at 1:1000 dilution.

Morphological analysis of organs

For isolation of organs, the preparation and section fixation of 7 μm sections was performed as described above. Classical heamatoxylin and eosin staining was performed as described previously (Mariotta *et al.* 2012).

Cloning of hLAT4 cDNA and cRNA synthesis

Human LAT4 cDNA in pTLN vector was kindly provided by Manuel Palacin (Bodoy *et al.* 2005). The construct was linearized using the *Bgl*II restriction site and cRNA

was synthesized using the MEGAscript high-yield *in vitro* transcription kit (Ambion, Austin, TX, USA) in accordance with the manufacturer's instructions.

Xenopus laevis oocytes preparation and cRNA injection

Stage IV oocytes (Dumont, 1972) were treated with collagenase A for 2–3 h at room temperature in Ca^{2+}-free buffer (82.5 mM NaCl, 2 mM $MgCl_2$, 10 mM Hepes, pH 7.4) and kept at 16°C in modified Barth's solution (88 mM NaCl, 1 mM KCl, 0.82 mM $MgSO_4$, 0.41 mM $CaCl_2$, 0.33 mM $Ca(NO_3)_2$, 2.4 mM $NaHCO_3$, 10 mM Hepes, 5 mg l^{-1} gentamicin, 5 mg l^{-1} doxycycline). Remaining follicular layers were manually removed. Next, 25 ng of LAT4 cRNA was injected and oocytes were incubated for 3 days at 16°C in ND96 solution (96 mM NaCl, 2 mM KCl, 1 mM $MgCl_2$, 1.8 mM $CaCl_2$, 5 mM Hepes-Tris, pH 7.4, supplemented with 50 mg l^{-1} tetracycline).

Uptake of AAs in *X. laevis* oocytes

Oocytes were washed six times with 2 ml of Na^+-buffer (100 mM NaCl, 2 mM KCl, 1 mM $CaCl_2$, 1 mM $MgCl_2$, 10 mM Hepes, pH 7.4) and then pre-warmed for 2 min at 25°C in a water bath. Subsequently, the pre-warming solution was aspirated and 100 μl of Na^+-buffer containing unlabelled phenylalanine at the indicated concentrations together with [^{3}H]-L-phenylalanine (10 μCi ml^{-1}) as tracer (Hartmann Analytic, Braunschweig, Germany) were added. Oocytes were then incubated for 10 min at 25°C. Thereafter, uptake solution was removed, oocytes were washed six times with 2 ml of ice-cold Na^+-buffer and separately dissolved in 250 μl of 2% SDS under agitation for at least 30 min. Upon the addition of 3 ml of scintillation fluid (Emulsifier-Safe), radioactivity was counted on a liquid scintillation counter (TRI-CARB 2900TR; Packard Instrument, Meriden, CT, USA). Uptake values were corrected by subtracting the values obtained from non-injected oocytes. Curves corresponding to the Michaelis–Menten equation were fitted to the data sets using GraphPad Prism, version 5.0 (GraphPad Software, San Diego, CA, USA).

Efflux of AAs in *X. laevis* oocytes

Oocytes were injected with 50 nl of different phenylalanine solutions (10 mM, 25 mM, 50 mM, 100 mM and 200 mM) together with [^{3}H]-L-phenylalanine (0.2 μCi μl^{-1}) as tracer. Assuming an oocyte volume of ~400 μl (Taylor & Smith, 1987), the resulting oocyte internal phenylalanine concentration upon injection corresponded, respectively, to 1.11 mM, 2.78 mM, 5.56 mM, 11.11 mM and 22.22 mM. Oocytes were subsequently washed four times in ND96 solution and 200 μl of ND96 were given to each oocyte. Efflux was allowed to take place for 10 min at 25°C before recovering the ND96 solution and washing the oocyte four times with ND96. Oocytes lysis and data analysis were conducted as for the uptake of AAs in *X. laevis* oocytes.

RNA extraction and real-time PCR

Mice at the indicated day after birth were killed by decapitation and organs were immediately rinsed several times with ice-cold PBS prior to being rapidly frozen in liquid propane until further use. Total RNA was extracted and reverse transcription was performed as described previously (Ramadan *et al.* 2006). For real-time PCR, 10 ng of cDNA template were used and the reaction was set in accordance with the manufacturer's instructions (TaqMan® Universal PCR master mix; Applied Biosystems, Foster City, CA, USA). The abundance of target mRNAs was standardized relative to 18S ribosomal RNA. Primers and probes for Lat2 (*Slc7a8*), 4F2hc (*Slc3a2*), y^+Lat1 (*Slc7a7*), y^+Lat2 (*Slc7a6*), Asct2 (*Slc1a5*), Tat1 (*Slc16a10*) and B^0AT1 (*Slc6a19*) were described previously (Moret *et al.* 2007; Mariotta *et al.* 2012). For Lat4 detection, the primers and probe used were: 5′-GCTGATTGCATATGGAGCAAGTAAC-3′ (forward), 5′-CGAAGTGAACGTCATGCACAT-3′ (reverse) and 5′-CTCTCTGTGCTCATCTTTATCGCCTTGGC-3′. For Eeg1 detection, the primers and probe used were: 5′-GCTACATCTTTGACCGCTTCAA-3′ (forward), 5′-CGCAGGTGTAGAAAAATATGGCTAT-3′ (reverse) and 5′-ACTACTGTGGCCCGCC-3′ (probe). For Lat3 detection, the primers and probe used were: 5′-CCCTGAATGAGAATGCTTCCTT-3′ (forward), 5′-ATGGCATTGGTGAGCTTTTGT-3′ (reverse) and 5′-AGCACCAAGTTCACTAGACCACGCTACCG-3′ (probe).

Isolation of pups at embryonic day 18 (E18) and measurements of AAs in amniotic fluids

Slc43a2$^{+/-}$ pregnant females were killed by cervical dislocation and amniotic sacs were dissected using standard laparotomy. Amniotic fluids were collected by puncturing the amniotic sacs and AA measurements were performed as described previously (Mariotta *et al.* 2012). E18 pups were subsequently isolated from their amniotic sacs and weighed.

Plasma AA and acylcarnitine measurements

Amino acids and acylcarnitines were measured after extraction with methanol without derivatization (Neobase Kit; Perkin Elmer, Turku, Finnland) on an Acquity-TQD

tandem mass spectrometer (Waters, Milford, MA, USA). Briefly, 3 μl of plasma were spotted onto pre-punched plain filter paper (Ahlstom 226; Perkin Elmer) in 96-well plain uncoated microtiter plates. Amino acids and acylcarnitines were extracted with 100 μl of methanolic extraction solution containing stable isotope labelled internal standards by shaking for 45 min at 45°C. Next, 30 μl of extract were then injected with a flow rate of 10 μl min^{-1} directly into the tandem mass spectrometer and measured afterwards in multiple reaction monitoring mode.

RNA-sequencing analysis of liver

Organs were isolated and RNA was extracted as described above. The quality of the isolated RNA was determined with a Qubit (1.0) Fluorometer (Life Technologies) and a Bioanalyzer 2100 (Agilent, Waldbronn, Germany). Only those samples with a 260 nm/280 nm ratio between 1.8 and 2.1 and a 28S/18S ratio in the range 1.5–2 were processed further. The TruSeq RNA Sample Prep Kit, version 2 (Illumina, Inc., Hayward, CA, USA) was used in the successive steps. Briefly, total RNA samples (100–1000 ng) were polyA enriched and then reverse-transcribed into double-stranded cDNA. The cDNA samples were fragmented, end-repaired and polyadenylated before ligation of TruSeq adapters containing the index for multiplexing. Fragments containing TruSeq adapters on both ends were selectively enriched with PCR. The quality and quantity of the enriched libraries were validated using a Qubit (1.0) Fluorometer and the Caliper GX LabChip GX (Caliper Life Sciences, Inc., Hopkinton, MA, USA). The product is a smear with an average fragment size of ~260 bp. The libraries were normalized to 10 nM in Tris-Cl 10 mM (pH 8.5) with 0.1% Tween 20. The TruSeq PE Cluster Kit v3-cBot-HS or TruSeq SR Cluster Kit v3-cBot-HS (Illumina, Inc.) was used for cluster generation using 10 pM of pooled normalized libraries on the cBOT. Sequencing were performed on the Illumina HiSeq 2000 paired end at 2 × 101 bp or single end 100 bp using the TruSeq SBS Kit v3-HS (Illumina, Inc.). RNA-sequencing reads were quality-checked with fastqc (www.bioinformatics.babraham.ac.uk/projects/fastqc), which computes various quality metrics for the raw reads. Reads were aligned to the genome and transcriptome with Tophat, version 1.3.3 (ccb.jhu.edu/software/tophat/index.shtml). Before mapping, the low quality ends of the reads were clipped (three bases from the read start and 10 bases from the read end). Tophat, version 1.3.3, was run with default options. The fragment length parameter was set to 100 bases with a standard deviation of 100 bases. Based on these alignments, the distribution of the reads across genomic features was assessed. Isoform expression was quantified with the RSEM algorithm (www.biomedcentral.com/1471-2105/12/323) with the option for estimation of the read start position distribution turned on. Raw data are available on the NCBI BioProject platform (www.ncbi.nlm.nih.gov/bioproject/) under the BioProject ID: PRJNA226691.

Determination of radiolabelled leucine and lysine distribution after oral administration

Mice at day 3 after birth were starved for 30 min in a humidified chamber on a warming plate set at 37°C. Subsequently, 5 μl of radiolabelled AA solution (1 mM leucine, [^{3}H]-L-leucine 0.2 μCi μl^{-1}, 1 mM lysine, [^{14}C]-L-lysine 0.04 μCi μl^{-1}) was administered and the mouse was placed in the chamber again for 30 min. Thereafter, mice were killed by decapitation and plasma was collected as described before. Organs were isolated, rinsed several times with ice-cold PBS and weighed. Subsequently, organs were lysed in Solvable (Perkin Elmer) overnight at 50°C and bleached with 200 μl of 30% H_2O_2. Radioactivity was determined upon addition of 12 ml of Ultima Gold scintillation liquid (Perkin Elmer) as described before (Mariotta *et al.*, 2012). AA accumulation within each organ was normalized to organ weight.

Blood glucose measurement

Mice at day 2 were killed by decapitation and blood glucose was measured with reactive test stripes Accu-Check (Roche Diagnostics, Mannheim, Germany).

Results

Lat4 protein absence in *Slc43a2*$^{-/-}$ mice and localization in wild-type mice epithelia

The expression and localization of the Lat4 protein was investigated using a new antibody that was validated by western blotting (data not shown). Immunofluorescence images of the small intestine and kidney proximal tubule of 3-day-old pups confirmed the absence of Lat4 protein in *Slc43a2* null pups compared to wild-type littermates (Fig. 1*A*–*D*). The integrity of the KO tissues showing no Lat4 signal was demonstrated by co-labelling with specific markers; for example, Tmem27 for kidney and MDR1 for liver (Fig. 1*A*, *B*, *G* and *H*). The lack of Lat4 signal in *Slc43a2* null mice additionally demonstrated the specificity of the immunofluorescence signals that localized to the basolateral membrane of kidney tubule (Fig. 1*A*) and small intestine (Fig. 1*C*) epithelial cells. As expected based on previous mRNA data (Bodoy *et al.* 2005), Lat4 expression was not detected in skeletal muscle and liver of wild-type and KO pups (Fig. 1*E*–*H*).

A strong Lat4-specific labelling was detected on small intestine villi at the basolateral membrane of enterocytes, whereas no clearly specific Lat4 signal was visible in the crypts (Fig. 2*A* and *B*). To investigate the localization of Lat4 along the mouse kidney nephron in more detail, we performed co-stainings or stainings of consecutive sections with tubule-specific markers. The strong expression of Lat4 in the proximal tubule was confirmed by labelling of the luminal SLC6-transporter accessory protein Tmem27 (Fig. 2*C*) and the aromatic AA uniporter Tat1 (consecutive sections Fig. 2*D* and *E*) in the same cells (Danilczyk *et al.* 2006; Ramadan *et al.* 2006). A weaker expression of Lat4 was detected in the distal convoluted tubule, which was co-stained with apical NCC antibody (Fig. 2*F*), whereas a strong expression of Lat4 was revealed in the thick-ascending limb of the loop of Henle, which was identified by NKCC2 labelling in a consecutive section (Fig. 2*G* and *H*) (Wagner *et al.* 2008). Taken together, our immunofluorescence data show that Lat4 protein is expressed at the basolateral membrane of

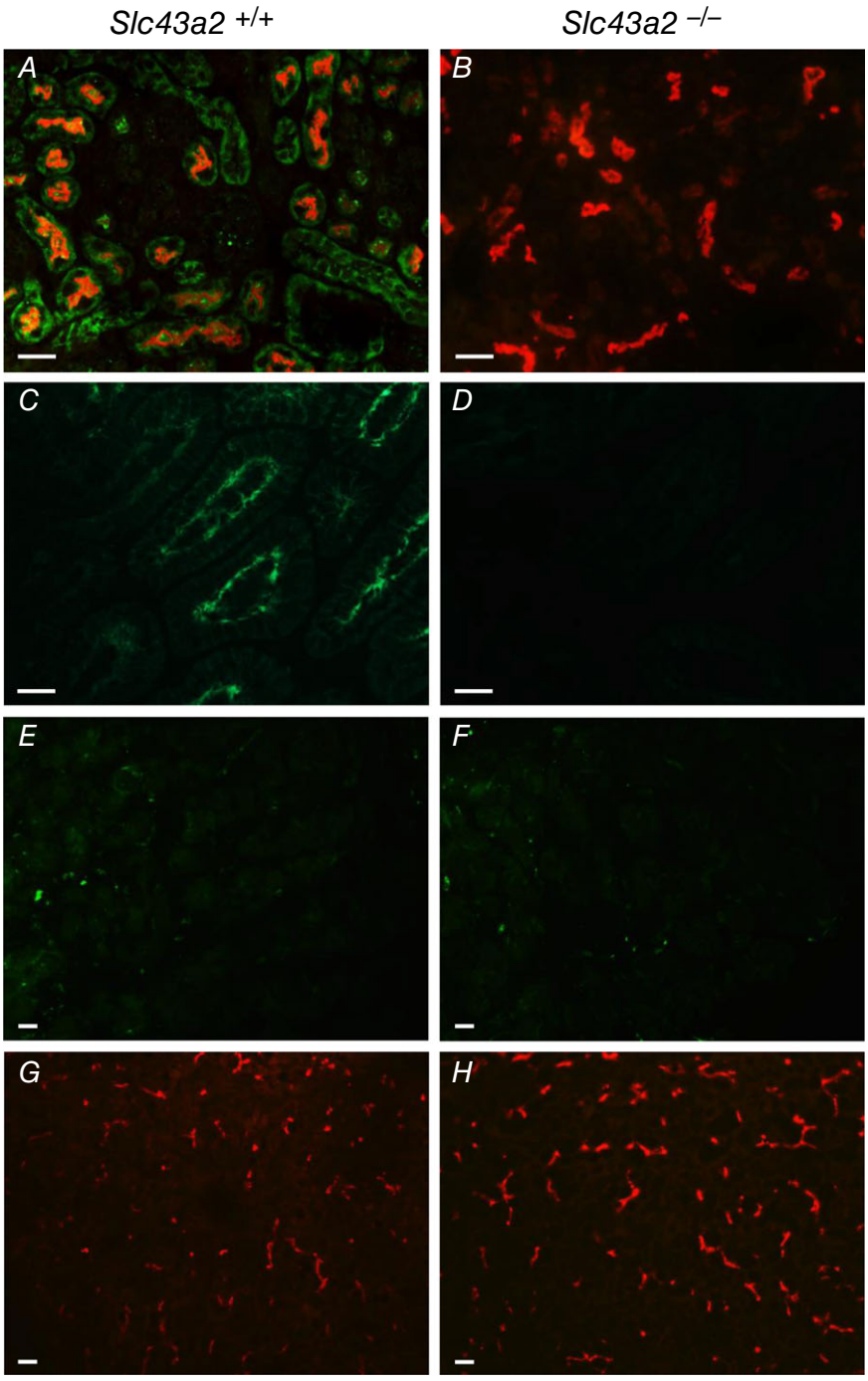

Figure 1. Confirmation of Lat4 deletion and validation of Lat4 antibody by immunofluorescence on tissue of wild-type and Lat4 KO pups
A basolateral signal is seen with Lat4 antibody (green) in the kidney (*A*) and small intestine (*C*) of 3-day-old wild-type pups, whereas no such signal is visible on sections from KO littermates (*B* and *D*). No signal (green) is observed in skeletal muscle (*E*) and liver (*G*) of wild-type pups in addition to the background also visible in the KO mice (*F* and *H*). As a luminal marker, Tmem27 (red) was used for kidney proximal tubule cells (*A* and *B*) and MDR1 was used for the canalicular membrane of liver hepatocytes (red) (*G* and *H*). Scale bars = 20 μm.

small intestine enterocytes, the kidney proximal tubule, thick ascending limb and, to a minor extent, of distal convoluted tubule epithelial cells.

Kinetic properties of LAT4 expressed in *X. laevis* oocytes

Originally, Lat4 was suggested to function as a uniporter based on the observation that it facilitated the efflux of phenylalanine from *X. laevis* oocytes independent of extracellular AAs (Bodoy *et al.* 2005). To determine the kinetic properties of Lat4, we performed a series of uptake and efflux rate measurements with different concentrations of phenylalanine using the *X. laevis* oocytes expression system (Fig. 3). Fitting Michaelis–Menten kinetics curves to the experimental phenylalanine uptake results, we derived the Michaelian constant ($K_{0.5}$) of 5.2 ± 0.5 mM (R^2 = 0.89). This value corresponded to

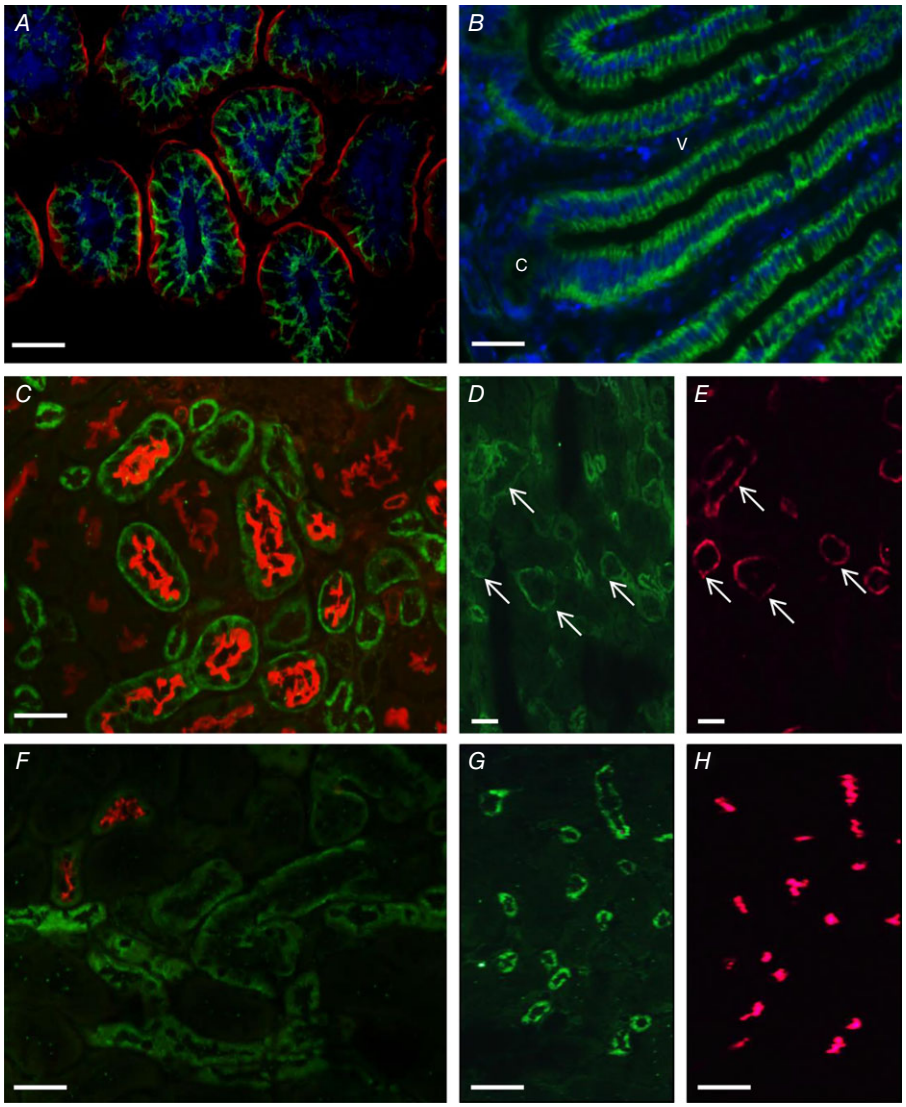

Figure 2. Localization of Lat4 on small intestine and kidney sections by immunofluorescence
A, on this cross-section of duodenal villi, Lat4 signal (green) localizes to the basolateral membrane of the enterocytes that are counterstained for the luminal transporter B^0AT1 (red). *B*, on a sagittal section of duodenal villi, Lat4 signal (green) is visible all along the villi (V) but not in crypts (*C*). In both (*A*) and (*B*), 4′,6-diamidino-2-phenylindole (blue) was used to label the nuclei. On kidney sections, Lat4 (green) signal is detectable in the proximal tubule (PT) which is identified in (C) by the luminal protein Tmem27 and by the basolateral uniporter Tat1 (pink) on consecutive sections (*D* and *E*). *F*, labelling of the luminal transporter NCC (red) identifies the distal convoluted tubule (DCT), which displays a weaker Lat4 signal compared to the proximal tube. *G* and *H*, a strong Lat4 signal (green) is visible in the thick ascending limb (TAL), which is identified in consecutive sections by the luminal transporter NKCC2 (red). Scale bar = 20 μm.

a low-affinity transport comparable to that previously reported by Bodoy *et al.* (2005) but no additional high-affinity/low capacity component was detected (Fig. 3*A*). To determine the efflux kinetic properties, oocytes were injected with increasing concentrations of phenylalanine and the resulting intracellular concentration of phenylalanine was estimated assuming an oocyte volume of 400 nl, as described previously (Meier *et al.* 2002). Fitting the Michaelis–Menten kinetics to the efflux values measured after 10 min yielded a low-affinity $K_{0.5}$ of 6.0 ± 1.4 mM ($R^2 = 0.66$), which was comparable to the apparent affinity value obtained for the uptake (Fig. 3*B*). Based on these results, we concluded that Lat4 shows symmetric intracellular and extracellular apparent affinities for phenylalanine.

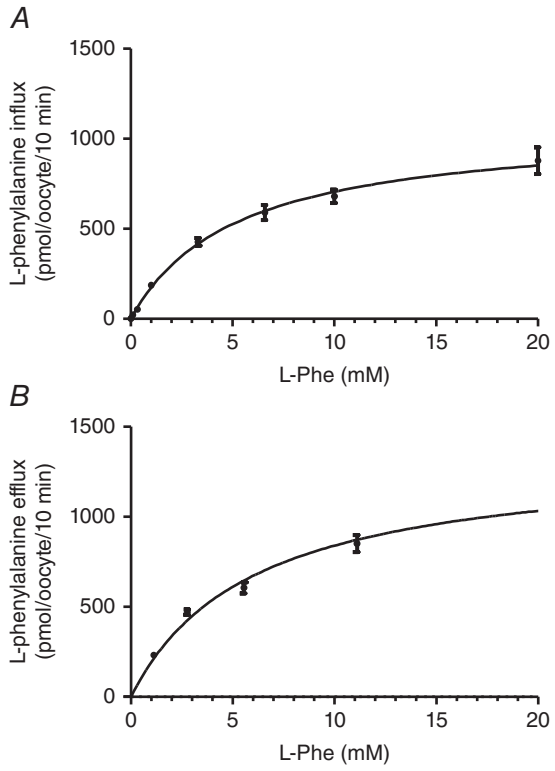

Figure 3. Concentration-dependence of L-phenylalanine uptake and efflux in *X. laevis* oocytes expressing human LAT4
Oocytes were injected with 25 ng of hSLC43A2 cRNA and incubated for 3 days. *A*, concentration-dependent uptakes were performed for 10 min with nine different concentrations of phenylalanine; $n = 8$–24 oocytes pooled from three independent experiments. *B*, for the efflux experiments, oocytes were injected with 50 nl of phenylalanine at five different concentrations; $n = 12$–14 oocytes pooled from three independent experiments. Data are the are mean ± SEM. Curves corresponding to the Michaelis–Menten equation were fitted to the experimental data using a non-linear regression routine (GraphPrism, version 5.0).

Intrauterine growth restriction and reduced amniotic fluid AA concentrations in Slc43a2$^{-/-}$ mice

Lat4 is known to be expressed in mouse placenta (Bodoy *et al.* 2005), where it might play an important role in AA transport, in particular by cooperating with the anti-porter Lat2–4F2hc (Cleal *et al.* 2011). To investigate the role of Lat4 in placental AA transport and intrauterine development, we analysed fetuses isolated from *Slc43a2*$^{+/-}$ *inter se* crossed mice at E18 (Fig. 4). *Slc43a2*$^{-/-}$ fetuses displayed a weight reduction of ∼10% compared to *Slc43a2*$^{+/+}$ and *Slc43a2*$^{+/-}$ littermates (E18 mean weight of ∼0.82 g for *Slc43a2*$^{-/-}$ *versus* 0.93 g for *Slc43a2*$^{+/+}$) (Fig. 4*B*) but no additional obvious phenotypical sign (Fig. 4*A*). This reduced intrauterine growth did not result in prenatal lethality because the birth statistics of *Slc43a2*$^{-/-}$ mice did not differ from the expected Mendelian ratio ($P = 0.48$, χ^2 test with $N > 100$ pups). To determine the effect of Lat4 deletion on placental AA transport, we measured the AA concentration in the amniotic fluid of individual pups (Fig. 4*C*). Interestingly, *Slc43a2*$^{-/-}$ mice displayed a marked reduction (i.e. > 50% compared to *Slc43a2*$^{+/+}$) in the concentration of almost all AAs, with the exception of aspartate and glutamate that did not show a statistically significant change. Measurements of other parameters, such as glucose and total protein concentration or osmolarity, did not show any difference (data not shown), pointing towards a specific defect of fetal AA supply. Therefore, we concluded that the lack of Lat4 results in a defective fetal AA delivery, which is not only restricted to Lat4-specific substrates but includes most AAs. These findings suggested that the defective Lat4 transport had led prenatally to a general decrease of AA-related transport, resulting in reduced intrauterine growth.

Growth defect, metabolic alterations and early postnatal lethality of *Slc43a2*$^{-/-}$ mice

Despite the reduced intrauterine growth reported above, *Slc43a2*$^{-/-}$ pups showed no pathological sign at birth. They displayed a normal skin colour and the presence of a white area at the left side of the abdomen (i.e. the so-called 'milk spot' confirmed normal milk delivery by the mother). However, monitoring of the postnatal weight revealed that *Slc43a2*$^{-/-}$ pups gained only very little weight compared to littermates (Fig. 5*A* and *B*). Furthermore, they all died within few days after birth, as shown in the Kaplan–Meier survival analysis (Fig. 5*C*). Indeed, more than 50% of the observed *Slc43a2*$^{-/-}$ pups died until postnatal day 7 and mortality reached 100% at day 10.

To obtain more information about the possible pathophysiological mechanisms underlying the early lethality, we measured the concentration of AAs in the plasma of 3-day-old *Slc43a2*$^{-/-}$ pups and compared this with age-matched littermates (Fig. 6*A*). We observed

a major decrease of certain AAs in *Slc43a2*$^{-/-}$ mice compared to *Slc43a2*$^{+/+}$. The highest relative difference was observed for non-essential AAs that are not substrates of Lat4 (e.g. proline with ~75% reduction followed by histidine, serine and alanine). Also Lat4 substrates appeared to be reduced in *Slc43a2*$^{-/-}$ mice [methionine strongly (> 50%) and branched-chain AAs less], although their decrease was not statistically significant. The only Lat4 substrate that did not appear to be decreased was phenylalanine. Thus, in analogy to the previous AA measurements in amniotic fluids, this blood AA pattern does not reflect a specific lack of Lat4 substrates but results

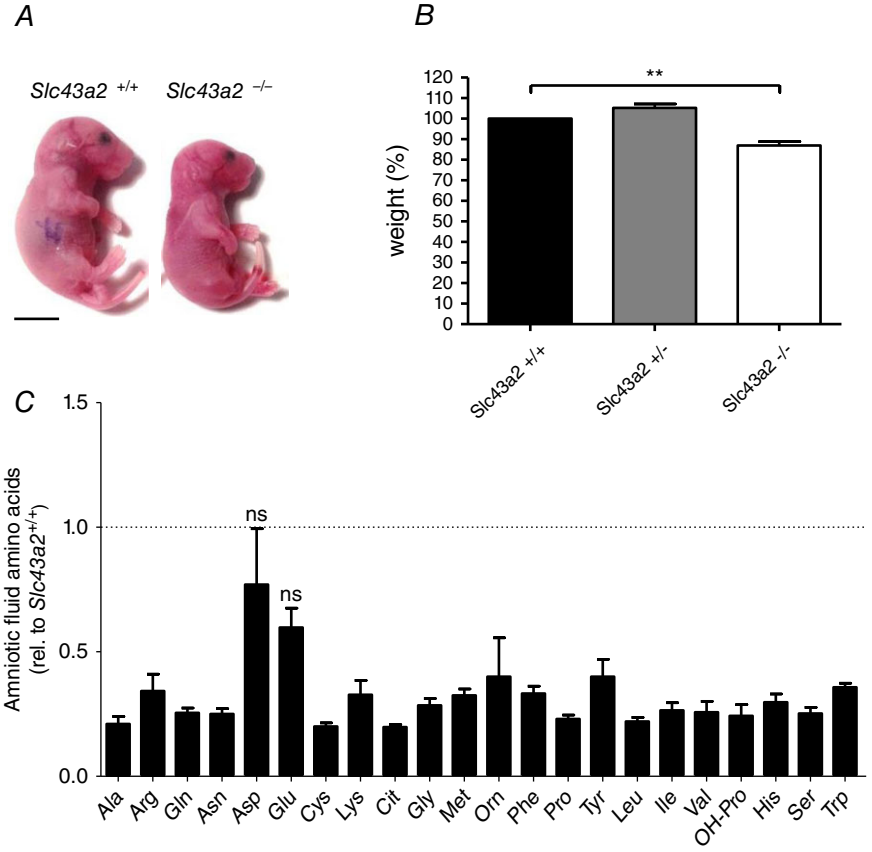

Figure 4. Effect of *Slc43a2* deletion on intrauterine growth and AA concentrations in amniotic fluid at E18
A, representative image of E18 *Slc43a2*$^{+/+}$ and *Slc43a2*$^{-/-}$ fetuses with corresponding weights. Scale bar = 5 mm. *B*, AA concentrations in amniotic fluids (*C*). Results were normalized to *Slc43a2*$^{+/+}$ (1.0) and represent the mean ± SEM of data pooled from two independent experiments: $n = 7$ for *Slc43a2*$^{+/+}$ mice, $n = 15$ for *Slc43a2*$^{+/-}$ mice and $n = 4$ for *Slc43a2*$^{-/-}$ mice. Two-way ANOVA and Dunnet's multiple comparison *post hoc* test for (*B*) and Bonferroni *post hoc* test for (*C*): $^{**}P < 0.01$. NS, non-significant.

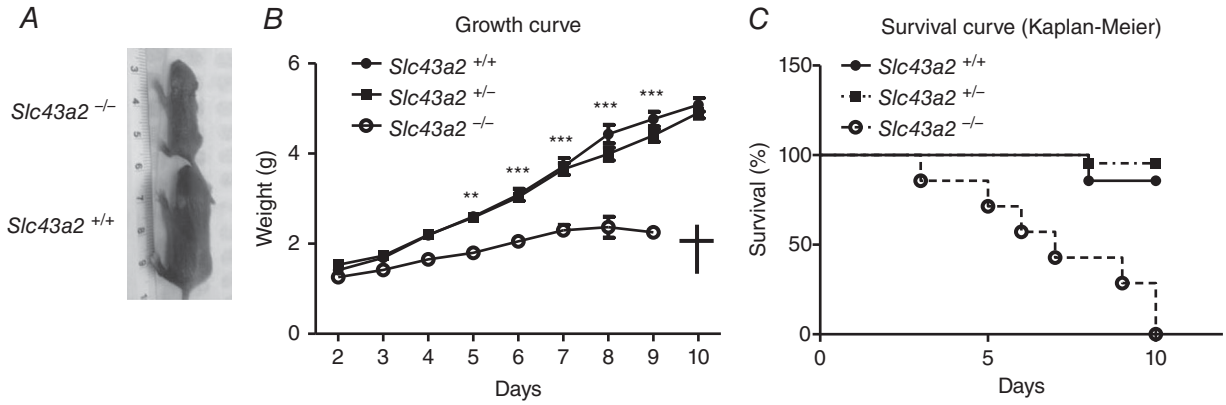

Figure 5. Postnatal growth retardation and premature death *of Slc43a2*$^{-/-}$ mice
A, representative image of a *Slc43a2*$^{-/-}$ mouse (top) *versus* a *Slc43a2*$^{+/+}$mouse (bottom) at day 7 after birth. *B*, growth curves for *Slc43a2*$^{+/+}$, *Slc43a2*$^{+/-}$ and *Slc43a2*$^{-/-}$ mice; represented as the mean ± SEM: $n = 7$ for *Slc43a2*$^{+/+}$, $n = 22$ for *Slc43a2*$^{+/-}$ and $n = 7$ for *Slc43a2*$^{-/-}$; comparison of *Slc43a2*$^{+/+}$ and *Slc43a2*$^{-/-}$. Two-way ANOVA and Bonferroni *post hoc* test: $^{**}P < 0.01$, $^{***}P < 0.001$; the cross represents the death of all *Slc43a2*$^{-/-}$ mice. *C*, survival curves for the same mice as (*B*).

probably from the interplay of transport and metabolic pathways that are altered in the *Slc43a2*$^{-/-}$ mice. In addition to the decrease in plasma AAs, we detected an increase of plasma acylcarnitine-conjugated fatty acids, in particular of dicarboxylic acids and long chain unsaturated fatty acids, which also highlighted a state of malnutrition (Fig. 6*C* and *D*). With regard to glucose homeostasis, *Slc43a2*$^{-/-}$ mice killed at day 2 showed a high blood concentration variability compared to *Slc43a2*$^{+/+}$ and *Slc43a2*$^{+/-}$ mice (Fig. 6*B*). Based on the hypothesis that this variability was the result of the different feeding status of single animals and that *Slc43a2*$^{-/-}$ pups might display a defect in glucose disposal (impaired insulin release) and gluconeogenesis, we starved the pups for 30 min before death and blood collection (Fig. 6*E*). Indeed, under these conditions, all *Slc43a2*$^{-/-}$ mice displayed a reduction in blood glucose concentration of ∼50% compared to their wild-type littermates. For this and also all other tested parameters, heterozygous *Slc43a2*$^{+/-}$ mice showed no difference compared to their *Slc43a2*$^{+/+}$ littermates.

Because *Slc43a2*$^{-/-}$ pups displayed a failure to grow and signs of malnutrition, we attempted to rescue them. We considered that an early defect in weight gain might represent a competitive disadvantage for obtaining breastfeeding within a large litter. Accordingly, we decreased this potential disadvantage by removing all *Slc43a2*$^{+/-}$ littermates on day 3, leaving only an equal number of *Slc43a2*$^{+/+}$ and *Slc43a2*$^{-/-}$ pups. However, *Slc43a2*$^{-/-}$ mice neither grew, nor survived better, even by reducing the litter size (data not shown). Moreover, we attempted to compensate malnutrition by S.C. administration of an AA-containing solution (Aminoven 10%, Fresenius KABI, 80 μl injection twice a day); however, this intervention resulted in no increase in weight gain or the lifespan of *Slc43a2*$^{-/-}$ mice.

Liver morphology and gene expression of *Slc43a2* null pups

Because the liver plays a central role in nutrients metabolism, we investigated the possible impact of *Slc43a2* defect on its morphology and gene expression pattern. Histological staining indeed showed sites of leucocyte infiltration in its periportal regions (Fig. 7*B*). Liver RNA-sequencing identified 16 078 transcripts as 'present' (Tophat software), with 1433 displaying a statistically significant ($P < 0.01$) differential expression (Fig. 7*A*).

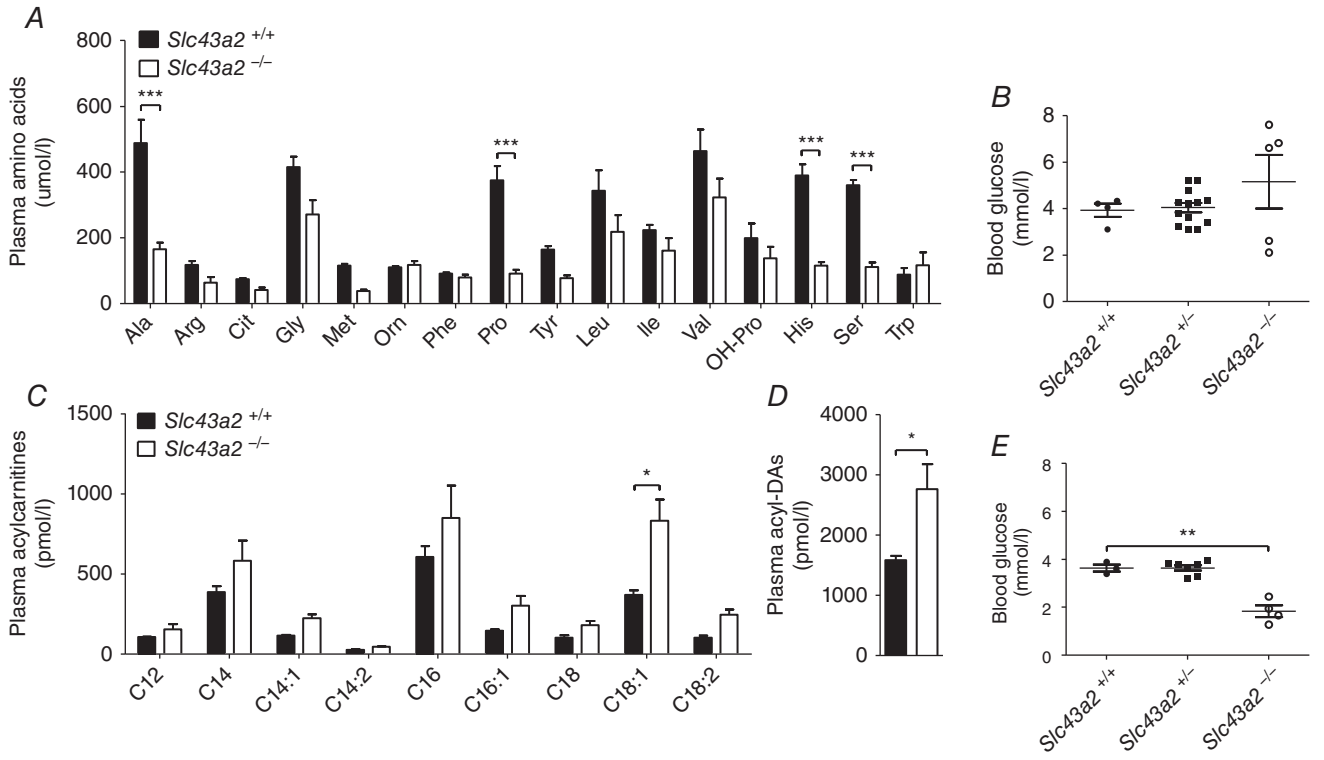

Figure 6. Impact of *Slc43a2* deletion on plasma AAs, acylcarnitines and glucose
Plasma AAs (*A*), long-chain unsaturated acylcarnitines (*C*) and dicarboxylacylcarnitines (DAs) (*D*). Represented are the mean ± SEM: $n = 3$ for *Slc43a2*$^{+/+}$ (black bars) and $n = 6$ for *Slc43a2*$^{-/-}$ (white bars). Two-way ANOVA and Bonferroni *post hoc* test: $^{*}P < 0.05$, $^{**}P < 0.001$. *B* and *E*, blood glucose measurement from mice at day 2 without (*B*) and with 30 min of starvation (*E*) prior to sample collection. Represented are the mean ± SEM. Student's *t* test: $^{**}P < 0.01$.

From these transcripts, the expression of 144 was changed by more than three-fold (77 increased and 67 decreased). Among the upregulated genes, many are known to be involved in liver regeneration (*Dmbt1*; Bisgaard *et al.* 2002), cell proliferation (*Htr2b*; Soll *et al.* 2010), tissue remodelling (*Mep1a* and *Mep1b*; Sterchi *et al.* 2008) and detoxification (*Gpx6 and Ggt6*; Gridley *et al.* 2011; Heisterkamp *et al.* 2008). Interestingly, the transcripts encoding acetyl-CoA carboxylase β (*Acab*), involved in lipogenesis (Postic & Girard, 2008), and glucokinase (*Gck*), involved in liver gluconeogenesis (Massa *et al.* 2011), were also upregulated. By contrast, genes involved in fatty acids biosynthesis, such as *Fas*, *Srbp1* and *Scd1* were not changed significantly. As expected based on the leucocyte infiltration, *Cyp2a5* and *Ceacam3* expression was increased (Sipowicz *et al.* 1997). The downregulation of the transcripts *Car3*, *Dio3* and *Inmt*, as well as of genes involved in hepatobiliary cholesterol excretion (*Abcg5* and *Abcg8*; Back *et al.* 2013) and the circadian clock (*Dbp*; Ando *et al.* 2011) similarly suggest major metabolic changes, inflammation, toxicity and regeneration at the level of the liver (Hsieh *et al.* 2009; Dudek *et al.* 2013) that might explain in part the increase in plasma fatty acids and the selective decrease of plasma AAs.

At the level of the kidney, which also plays an important role for the systemic metabolism of AAs (Makrides *et al.* 2014), we tested the expression of AA transporters but did not identify any major alterations in *Slc43a2*$^{-/-}$ mice (Fig. 7*C*). Interestingly, other AA transporters of the SLC43 family (i.e. Lat3 and Eeg1) showed no differential expression in *Slc43a2*$^{-/-}$ mice; therefore, the lack of Lat4 did not appear to result in any compensatory regulation of AA transporters with similar substrate affinities.

Accumulation of leucine in the proximal part of the small intestine

The major metabolic changes described above suggested that the early death of *Slc43a2*$^{-/-}$ mice might be a result of the status of malnutrition. Because we showed that Lat4 was expressed at the basolateral membrane of enterocytes (Fig. 2), we hypothesized that this malnutrition might result from a defective intestinal AA absorption. To test

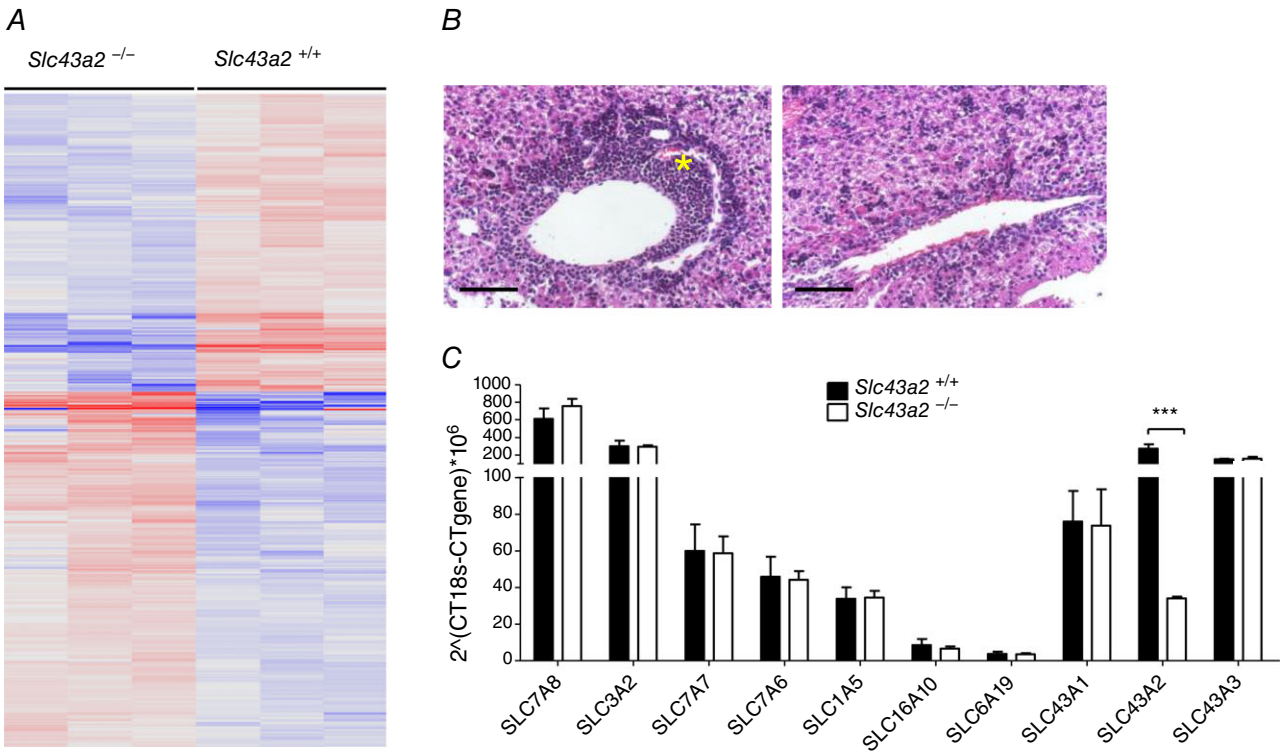

Figure 7. Effect of *Slc43a2* deletion on liver and kidney
A, heat map summary of differential gene expression pattern in *Slc43a2*$^{-/-}$ liver. RNA was isolated from mice at day 2 and each column represents a different mouse. Upregulated genes are indicated in red; downregulated genes are indicated in blue. *B*, heamatoxylin and eosin staining of liver. Left: liver section of *Slc43a2*$^{-/-}$ KO mouse. Right: liver section of *Slc43a2*$^{+/+}$ mouse. *Leucocyte infiltration in the periportal region of *Slc43a2*$^{-/-}$ mouse liver. Scale bar = 50 μm. *C*, gene expression of selected AA transporters in the kidney of *Slc43a2*$^{+/+}$ (black bars) and *Slc43a2*$^{-/-}$ (white bars). Represented are the mean ± SEM: $n = 3$. Two-way ANOVA and Bonferroni *post hoc* test: $^{**}P < 0.01$.

this hypothesis, we starved pups for 30 min and then fed them with 5 μl of an AA solution containing 1 mM of each leucine and lysine with corresponding ^{3}H and ^{14}C tracers. Leucine was chosen as Lat4 substrate because it is not transported by the other basolateral uniporter Tat1, whereas lysine was chosen because it is not transported by Lat4. Upon administration of this AA mixture, we monitored the appearance of the labelled AAs in plasma and their accumulation in different organs after 30 min (Fig. 8). Pups lacking Lat4 displayed a marked two-fold increased retention of leucine, but not of lysine, in the first part of the small intestine compared to wild-type littermates (Fig. 8*A* and *C*). This selective retention of the Lat4 substrate leucine in the small intestine of *Slc43a2*$^{-/-}$ pups suggested its intracellular retention in the absence of basolateral Lat4. This selective retention was not associated with a visible morphological difference as observed on haematoxylin and eosin stained small intestine sections. It also did not lead to differences in terms of AA appearance in plasma or levels in other organs after 30 min (Fig. 8*B* and *D*).

Discussion

Lat4 is considered a 'system L' transporter because it transports large neutral AAs independent of Na^{+}. This functional denomination, however, does not include other important transport characteristics such as transport type and affinity that clearly differentiate Lat4 from the classical system L transporters Lat1 and Lat2 (Lat1–4F2hc/*Slc7a5-Slc3a2* and Lat2–4F2hc/*Slc7a8-Slc3a2*). Indeed, as originally suggested by Bodoy *et al.* (Bodoy *et al.* 2005), Lat4 functions as a uniporter (facilitated diffusion pathway) and we show here that it does this with a low, symmetrical apparent affinity (Fig. 3). These functional characteristics contrast with those of the classical system L transporters Lat1 and Lat2 that function as asymmetric anti-porters with high apparent affinity for the uptake of their substrates (Meier *et al.* 2002). Additionally, the selectivity of Lat4 is more limited and includes only essential AAs, specifically the branched-chain ones plus phenylalanine and methionine. Because the *in vivo* role of this AA transporter has yet not been investigated, we further analysed its localization and tested its physiological function in the present study using a newly generated general KO mouse model.

The main observation reported here is that mice defective in Lat4 suffer from a small intrauterine growth restriction, a major postnatal growth defect and premature death within a few days after birth, despite normal feeding behaviour suggested by the 'milk spot'.

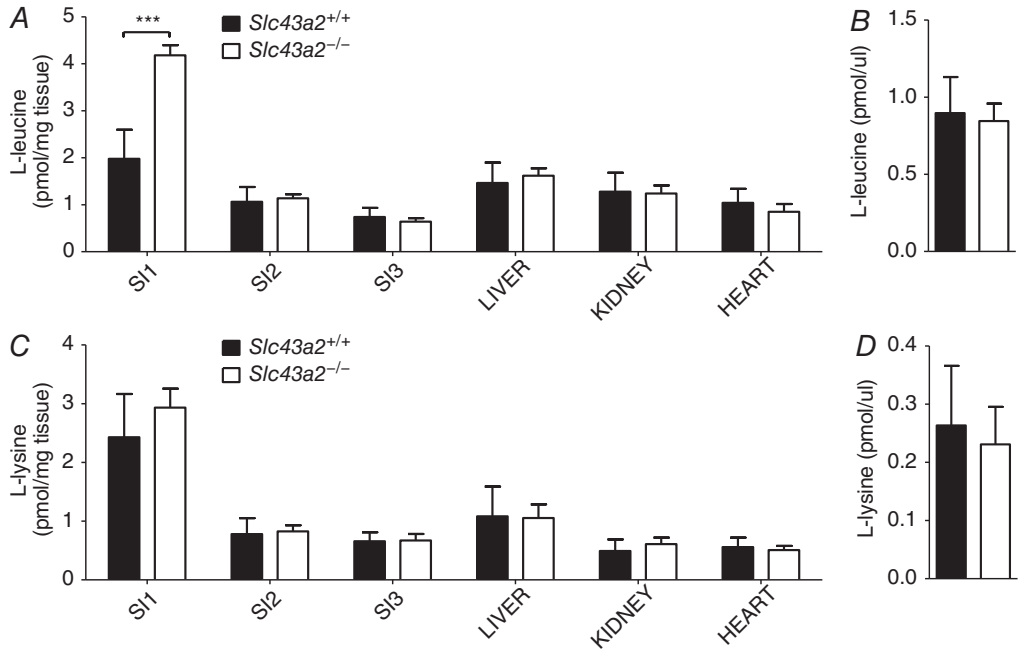

Figure 8. Distribution of radiolabelled L-leucine and L-lysine in different organs after oral administration
Mice were starved 30 min prior to oral administration of radiolabelled AA solution. Leucine (*A*) and (*C*) lysine accumulation in different organs normalized by weight. Leucine (*B*) and (*D*) lysine concentration in plasma 30 min after oral administration (*Slc43a2*$^{+/+}$: black bars, *Slc43a2*$^{-/-}$: white bars). The small intestine of the pups was divided into three equals parts from proximal to distal: SI1, SI2 and SI3. Represented are the mean ± SEM pooled from three independent experiments: $n = 6$ for *Slc43a2*$^{+/+}$ mice and $n = 8$ for *Slc43a2*$^{-/-}$ mice. Two-way ANOVA and Bonferroni *post hoc* test: $^{***}P < 0.001$.

The question is what functional defect is provoked by the lack of Lat4, which leads to this developmental problem? The phenotype does not appear to depend on the genetic background because it was not modified by backcrossing for six generations with C57BL/6 or S129 mice. Despite the fact that attempts to rescue the pups by litter size reduction (decreased competition) or parenteral nutritional supplementation did not succeed, this lethal phenotype is probably largely the result of a combination of defective placental and, in particular, intestinal AA transport that leads to severe postnatal malnutrition.

Lat4 is a basolateral uniporter for essential neutral AAs in the small intestine and kidney tubule

A first crucial aspect towards understanding the function of Lat4 is its tissue and subcellular localization. In the original study by Bodoy *et al.* (2005), which reported its identification and mRNA expression in human and mouse tissues, Lat4 mRNA was shown to be present at high levels in placenta, kidney and small intestine, as well as at lower levels in several other tissues and in a proximal tubule cell line. Additionally, expression data from available microarray analysis (www.biogps.com) indicate a strong expression in macrophages, microglia and osteoclasts. As previously hypothesized, we now show, using a newly generated antibody, that Lat4 localizes to the basolateral membrane of AA transporting cells of small intestine and kidney proximal tubule. Furthermore, we confirm the selectivity of the staining at these locations using the KO mouse model. These images show that Lat4 is expressed in the small intestine at a much higher level in the villi than in the crypts, similar to other AA transporters involved in transepithelial transport (Fig. 2*A* and *B*) (Dave *et al.* 2004). These data strongly support the hypothesis that Lat4 plays an important role for the (re)absorption of AAs. Interestingly, in the kidney, in addition to a strong labelling in the proximal tubule (Fig. 2*C–E*), there is also a strong basolateral labelling in the thick ascending limb of the loop of Henle and a weaker signal in the distal convoluted tubule (Fig. 2*F–H*). The low level or absence of Lat4 protein expression in liver and skeletal muscle suggested by previous mRNA data is also confirmed by our immunofluorescence results (Fig. 1*E–H*).

As demonstrated in the present study with expression experiments in *X. laevis* oocytes, Lat4 is a symmetrical uniporter with a low affinity for its substrates (Fig. 3). Thus, at physiological substrate concentrations, its directional transport activity is proportional to the transmembrane substrate concentration difference. This allows Lat4, if expressed at a sufficiently high level, to mediate the equilibration of its AA substrates (branched-chain AAs, phenylalanine and methionine) between the extracellular space and the cytosol. It can thus mediate a directional transport of its substrates across the plasma membrane; for example, their basolateral efflux from small intestine and kidney proximal tubule cells after their luminal uptake from the intestinal lumen or primary urine. We postulate that this directional basolateral efflux transport also represents a recycling pathway for AAs that are taken up across the same basolateral membranes with high affinity by the parallel localized heterodimeric anti-porters *Slc7a8-Slc3a2*/Lat2–4F2hc and *Slc7a7-Slc3a2*/y^+Lat1–4F2hc. Such a high affinity uptake of essential AAs by these anti-porters allows them to efflux in exchange non-essential AAs present mostly at much a higher concentration than the essential AAs in these epithelial cells. Thus, Lat4 may exert a quantitative control of the Lat2 and y^+Lat1 anti-porter efflux activity by recycling the essential AAs that they take up in exchange to the outside. Correspondingly, the expectation is that the lack of Lat4 could affect the transepithelial transport of other, in particular non-essential and cationic AAs. Such a functional relationship/cooperation with anti-porters for the efflux of non-essential AAs has previously been demonstrated in the *X. laevis* oocyte expression system and *in vivo* for the aromatic AA transporter Tat1, another essential AA uniporter expressed at the basolateral membrane of transporting epithelial cells (Ramadan *et al.* 2007; Mariotta *et al.* 2012). However, in the present case, functional experiments aiming to test the impact of Lat4 defect on the transport of AAs were strongly limited by the fact that Lat4 mice did not develop normally and died a few days after birth.

Concerning Lat4 localization, an intriguing observation was that Lat4 is expressed at a high level also in the kidney thick ascending limb, as previously reported at the mRNA level (Cheval *et al.* 2011). We postulated that the basolateral expression of Lat4 in these cells plays a role with respect to energy metabolism and/or for the synthesis of the highly abundant secreted surface protein uromodulin (Glaudemans *et al.* 2014) rather than for the transepithelial transport of AAs. These cells might thus import branched-chain AAs and methionine via Lat4 for use in protein synthesis and as catabolic substrates for the production of ATP or to drive the influx of non-essential AAs, such as glutamine, which then function as metabolic fuel (opposite net transport direction compared to transepithelial transport).

Prenatal and postnatal failure to grow, malnutrition and death of *Slc43a2*$^{-/-}$ KO mice

The global disruption of the AA uniporter Lat4 highlighted the pivotal importance of this AA transporter in prenatal and postnatal development. *Slc43a2*$^{-/-}$ KO mice displayed defective growth before birth with an ∼10% reduction of weight at E18 compared to wild-type littermates. The

reported defective growth showed phenotypical analogies with other KO mouse models of AA transporters, such as y^+Lat1 and CAT-1 (Xie *et al.* 2005; Sperandeo *et al.* 2007), suggesting that Lat4 should be also considered together with the aforementioned AA transporters as a very important player in placental AA transport. Interestingly, Lat4 dysfunction resulted not only in a reduction of its AA substrates in the amniotic fluid, but also in a general decrease of all AAs, except for aspartate and glutamate. Thus, defective Lat4 function causes pleiotropic consequences that are not limited to a lack of Lat4-specific substrates but encompass many other AAs. The reduced weight and reduced concentration of AAs in the amniotic fluid neither resulted in prenatal lethality, nor disrupted the postnatal feeding behaviour as suggested by the presence of a normal 'milk spot'. However, as shown by the postnatal growth curve and the concentration of different metabolites in plasma of 3-day-old mice, it appeared they display a defect in enteric AA absorption that could be the origin of the postnatal growth defect and also contribute to a major extent to the premature lethality of *Slc43a2*$^{-/-}$ mice.

The metabolic status of the *Slc43a2*$^{-/-}$ pups already 3 days after birth showed many analogies with starvation. Initially, and unexpectedly, methionine was the only Lat4 substrate to be highly decreased in their plasma, whereas branched-chain AAs and phenylalanine showed only a minor reduction. By contrast, many non-essential AAs were markedly decreased, mostly alanine and proline. However, based on the suggested function of Lat4 as a 'gate keeper' for the epithelial basolateral efflux of non-essential AAs via anti-porters (see above), it is not unexpected that a *Slc43a2*$^{-/-}$-induced defect in AA absorption may lead to a catabolic state in which the decrease in non-essential AAs is more marked than that of essential ones (Fig. 9).

Non-essential AAs are also specifically decreased in fasted children (Wolfsdorf *et al.* 1982) and upon prolonged endurance exercise, particularly alanine and proline that are central for AA metabolism and gluconeogenesis (Ji *et al.* 1987; Huq *et al.* 1993). Also, the decrease in tyrosine, histidine and serine can be explained by their catabolic usage to provide substrates for the Krebs cycle. The increase in plasma acylcarnitine-conjugated dicarboxylic and long-chain unsaturated fatty acids in *Slc43a2*$^{-/-}$ mice is an additional metabolic fingerprint indicating that the *Slc43a2*$^{-/-}$ pups are in a state of starvation (Costa *et al.* 1999; Hunt & Alexson, 2002). Additionally, histological examination and the gene expression analysis of the liver, by indicating processes of inflammation, regeneration and alteration of glucose and fatty acids metabolism, further demonstrated that *Slc43a2* null pups suffered from malnutrition. Indeed, an alteration in glucose metabolism, which is a hallmark of nutritional defects in children (Bandsma *et al.* 2010; Spoelstra *et al.* 2012), was also present in *Slc43a2*$^{-/-}$ mice, as shown by the marked decrease in blood glucose concentration measured upon 30 min of starvation.

The hypothesis that Lat4 impacts on AA absorption was further supported by our observation that leucine administered orally was retained in the proximal part of the small intestine of *Slc43a2*$^{-/-}$ mice, unlike lysine, which is not a Lat4 substrate. This suggests that luminally absorbed leucine accumulated in small intestine enterocytes from which it could not be efficiently released basolaterally. However, no concomitant alteration in plasma appearance or organ accumulation of leucine was observed in these mice, such that a possible major defect in AA absorption from ingested food could not be verified. It is, however, possible that the non-physiological administration of two AAs at a high concentration (1 mM

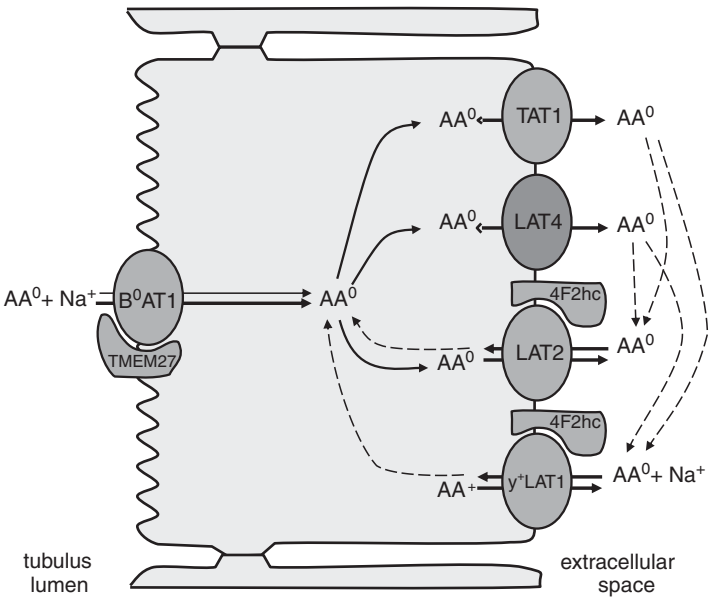

Figure 9. Schematic representation of apical and basolateral AA transporter cooperation in proximal tubule kidney cell
Neutral AAs are imported apically mostly via the symporter B^0AT1 (*SLC6A19*) and are effluxed across the basolateral membrane mostly by the anti-porter LAT2–4F2hc and the uniporters TAT1 and LAT4. We postulate that essential neutral AAs are equilibrated between the intracellular compartment and the extracellular space via the two low affinity uniporters TAT1 and LAT4 and may recycle into the cell via anti-porters and thereby drive the efflux of other AAs, in particular of (non)-essential neutral AAs via LAT2–4F2hc and cationic AAs via y^+LAT1–4F2hc. Therefore, a defect in the uniporter(s) LAT4 and/or TAT1 is suggested to impact not only on the basolateral efflux of their own AA substrates, but also on that of the other substrates of the anti-porters LAT2–4F2hc and y^+LAT1–4F2hc.

each) to a large extent bypassed a defect preventing the sufficient absorption from mother's milk. An additional untested possibility is that the AAs permanently secreted by the liver and the pancreas into the intestine lumen, as well as the AAs resulting from enterocyte shedding, were not efficiently reabsorbed, leading finally to a substantial AAs loss into the faeces.

An interesting observation is that, out of five KO mouse models lacking AA transporters expressed in the small intestine and kidney proximal tubule, the KO of Lat4 is only the second one that leads to a lethal phenotype. Neither the lack of luminal B^0AT1 transporter, nor the lack of the basolateral L-type anti-porter Lat2 (*Slc7a8*) and of the aromatic AA uniporter Tat1 (*Slc16a10*) prevents normal life and reproduction under laboratory conditions. The KO of Lat4 is the first AA transporter defect that, despite a normal Mendelian birth ratio, leads to a severe postnatal malnutrition with early death. Many of the observations reported in the present study suggest that the primary cause of *Slc43a2*$^{-/-}$ pups malnutrition may be a defect in AA absorption from the gut. However, it was not formally excluded that the observed malnutrition syndrome was partly the result of an insufficient suckling drive or another alteration preventing the appropriate use of mother's milk as a nutrition source.

In addition, we considered the possibility that Lat4 deficiency, because of its high expression in macrophages and microglia (www.biogps.org), could impact on the survival of the pups by affecting the immune system. However, transgenic mice with defective hematopoietic mononuclear phagocytic cells, such as *Csfr1*$^{-/-}$ KO (Dai *et al.* 2002) or *op/op* mice (Wiktor-Jedrzejczak *et al.* 1990), have been shown to survive beyond weaning, clearly indicating that the lethality of Lat4 KO mice is not the result of an immune defect.

In conclusion, we provide the first characterization of a total *Slc43a2* KO mouse model. The small intrauterine growth retardation and the postnatal malnutrition phenotype leading to an early death indicate that Lat4 is an essential AA transporter required for the proper placental AA transport and postnatal nutrient absorption.

References

Ando H, Kumazaki M, Motosugi Y, Ushijima K, Maekawa T, Ishikawa E & Fujimura A (2011). Impairment of peripheral circadian clocks precedes metabolic abnormalities in ob/ob mice. *Endocrinology* **152**, 1347–1354.

Babu E, Kanai Y, Chairoungdua A, Kim DK, Iribe Y, Tangtrongsup S, Jutabha P, Li Y, Ahmed N, Sakamoto S, Anzai N, Nagamori S & Endou H (2003). Identification of a novel system L amino acid transporter structurally distinct from heterodimeric amino acid transporters. *J Biol Chem* **278**, 43838–43845.

Back SS, Kim J, Choi D, Lee ES, Choi SY & Han K (2013). Cooperative transcriptional activation of ATP-binding cassette sterol transporters ABCG5 and ABCG8 genes by nuclear receptors including Liver-X-Receptor. *BMB Rep* **46**, 322–327.

Bandsma RH, Mendel M, Spoelstra MN, Reijngoud DJ, Boer T, Stellaard F, Brabin B, Schellekens R, Senga E & Heikens GT (2010). Mechanisms behind decreased endogenous glucose production in malnourished children. *Pediatr Res* **68**, 423–428.

Bisgaard HC, Holmskov U, Santoni-Rugiu E, Nagy P, Nielsen O, Ott P, Hage E, Dalhoff K, Rasmussen LJ & Tygstrup N (2002). Heterogeneity of ductular reactions in adult rat and human liver revealed by novel expression of deleted in malignant brain tumor 1. *Am J Pathol* **161**, 1187–1198.

Bodoy S, Martin L, Zorzano A, Palacin M, Estevez R & Bertran J (2005). Identification of LAT4, a novel amino acid transporter with system L activity. *J Biol Chem* **280**, 12002–12011.

Borsani G, Bassi MT, Sperandeo MP, De Grandi A, Buoninconti A, Riboni M, Manzoni M, Incerti B, Pepe A, Andria G, Ballabio A & Sebastio G (1999). SLC7A7, encoding a putative permease-related protein, is mutated in patients with lysinuric protein intolerance. *Nat Genet* **21**, 297–301.

Braun D, Wirth EK, Wohlgemuth F, Reix N, Klein MO, Gruters A, Kohrle J & Schweizer U (2011). Aminoaciduria, but normal thyroid hormone levels and signaling, in mice lacking the amino acid and thyroid hormone transporter Slc7a8. *Biochem J* **439**, 249–255.

Broer S & Palacin M (2011). The role of amino acid transporters in inherited and acquired diseases. *Biochem J* **436**, 193–211.

Camargo SM, Singer D, Makrides V, Huggel K, Pos KM, Wagner CA, Kuba K, Danilczyk U, Skovby F, Kleta R, Penninger JM & Verrey F (2009). Tissue-specific amino acid transporter partners ACE2 and collectrin differentially interact with hartnup mutations. *Gastroenterology* **136**, 872–882.

Cheval L, Pierrat F, Dossat C, Genete M, Imbert-Teboul M, Duong Van Huyen JP, Poulain J, Wincker P, Weissenbach J, Piquemal D & Doucet A (2011). Atlas of gene expression in the mouse kidney: new features of glomerular parietal cells. *Physiol Genomics* **43**, 161–173.

Cleal JK, Glazier JD, Ntani G, Crozier SR, Day PE, Harvey NC, Robinson SM, Cooper C, Godfrey KM, Hanson MA & Lewis RM (2011). Facilitated transporters mediate net efflux of amino acids to the fetus across the basal membrane of the placental syncytiotrophoblast. *J Physiol* **589**, 987–997.

Costa CC, de Almeida IT, Jakobs C, Poll-The BT & Duran M (1999). Dynamic changes of plasma acylcarnitine levels induced by fasting and sunflower oil challenge test in children. *Pediatr Res* **46**, 440–444.

Dai XM, Ryan GR, Hapel AJ, Dominguez MG, Russell RG, Kapp S, Sylvestre V & Stanley ER (2002). Targeted disruption of the mouse colony-stimulating factor 1 receptor gene results in osteopetrosis, mononuclear phagocyte deficiency, increased primitive progenitor cell frequencies, and reproductive defects. *Blood* **99**, 111–120.

Danilczyk U, Sarao R, Remy C, Benabbas C, Stange G, Richter A, Arya S, Pospisilik JA, Singer D, Camargo SM, Makrides V, Ramadan T, Verrey F, Wagner CA & Penninger JM (2006). Essential role for collectrin in renal amino acid transport. *Nature* **444,** 1088–1091.

Dave MH, Schulz N, Zecevic M, Wagner CA & Verrey F (2004). Expression of heteromeric amino acid transporters along the murine intestine. *J Physiol* **558,** 597–610.

Dudek KM, Suter L, Darras VM, Marczylo EL & Gant TW (2013). Decreased translation of Dio3 mRNA is associated with drug-induced hepatotoxicity. *Biochem J* **453,** 71–82.

Dumont JN (1972). Oogenesis in *Xenopus laevis* (Daudin). I. Stages of oocyte development in laboratory maintained animals. *J Morphol* **136,** 153–179.

Fickert P, Zollner G, Fuchsbichler A, Stumptner C, Pojer C, Zenz R, Lammert F, Stieger B, Meier PJ, Zatloukal K, Denk H & Trauner M (2001). Effects of ursodeoxycholic and cholic acid feeding on hepatocellular transporter expression in mouse liver. *Gastroenterology* **121,** 170–183.

Fukuhara D, Kanai Y, Chairoungdua A, Babu E, Bessho F, Kawano T, Akimoto Y, Endou H & Yan K (2007). Protein characterization of NA^+-independent system L amino acid transporter 3 in mice: a potential role in supply of branched-chain amino acids under nutrient starvation. *Am J Pathol* **170,** 888–898.

Glaudemans B, Terryn S, Gölz N, Brunati M, Cattaneo A, Bachi A, Al-Qusairi L, Ziegler U, Staub O, Rampoldi L & Devuyst O (2014). A primary culture system of mouse thick ascending limb cells with preserved function and uromodulin processing. *Pflügers Arch* **466,** 343–56.

Gridley DS, Freeman TL, Makinde AY, Wroe AJ, Luo-Owen X, Tian J, Mao XW, Rightnar S, Kennedy AR, Slater JM & Pecaut MJ (2011). Comparison of proton and electron radiation effects on biological responses in liver, spleen and blood. *Int J Radiat Biol* **87,** 1173–1181.

Heisterkamp N, Groffen J, Warburton D & Sneddon TP (2008). The human gamma-glutamyltransferase gene family. *Hum Genet* **123,** 321–332.

Hsieh HC, Chen YT, Li JM, Chou TY, Chang MF, Huang SC, Tseng TL, Liu CC & Chen SF (2009). Protein profilings in mouse liver regeneration after partial hepatectomy using iTRAQ technology. *J Proteome Res* **8,** 1004–1013.

Hunt MC & Alexson SE (2002). The role Acyl-CoA thioesterases play in mediating intracellular lipid metabolism. *Prog Lipid Res* **41,** 99–130.

Huq F, Thompson M & Ruell P (1993). Changes in serum amino acid concentrations during prolonged endurance running. *Jpn J Physiol* **43,** 797–807.

Ji LL, Miller RH, Nagle FJ, Lardy HA & Stratman FW (1987). Amino acid metabolism during exercise in trained rats: the potential role of carnitine in the metabolic fate of branched-chain amino acids. *Metabolism* **36,** 748–752.

Kaplan MR, Plotkin MD, Lee WS, Xu ZC, Lytton J & Hebert SC (1996). Apical localization of the Na-K-Cl cotransporter, rBSC1, on rat thick ascending limbs. *Kidney Int* **49,** 40–47.

Loffing J, Vallon V, Loffing-Cueni D, Aregger F, Richter K, Pietri L, Bloch-Faure M, Hoenderop JG, Shull GE, Meneton P & Kaissling B (2004). Altered renal distal tubule structure and renal Na(+) and Ca(2+) handling in a mouse model for Gitelman's syndrome. *J Am Soc Nephrol* **15,** 2276–2288.

Makrides V, Camargo SMR, and Verrey F (2014). Transport of amino acids in the kidney. *Comprehensive Physiology* **4,** 367–403.

Mariotta L, Ramadan T, Singer D, Guetg A, Herzog B, Stoeger C, Palacin M, Lahoutte T, Camargo SM & Verrey F (2012). T-type amino acid transporter TAT1 (Slc16a10) is essential for extracellular aromatic amino acid homeostasis control. *J Physiol* **590,** 6413–6424.

Massa ML, Gagliardino JJ & Francini F (2011). Liver glucokinase: an overview on the regulatory mechanisms of its activity. *IUBMB Life* **63,** 1–6.

Meier C, Ristic Z, Klauser S & Verrey F (2002). Activation of system L heterodimeric amino acid exchangers by intracellular substrates. *EMBO J* **21,** 580–589.

Moret C, Dave MH, Schulz N, Jiang JX, Verrey F & Wagner CA (2007). Regulation of renal amino acid transporters during metabolic acidosis. *Am J Physiol Renal Physiol* **292,** F555–F566.

Nassl AM, Rubio-Aliaga I, Sailer M & Daniel H (2011). The intestinal peptide transporter PEPT1 is involved in food intake regulation in mice fed a high-protein diet. *PLoS One* **6**, e26407.

Poncet N & Taylor PM (2013). The role of amino acid transporters in nutrition. *Curr Opin Clin Nutr Metab Care* **16**, 57–65.

Postic C & Girard J (2008). Contribution of de novo fatty acid synthesis to hepatic steatosis and insulin resistance: lessons from genetically engineered mice. *J Clin Invest* **118**, 829–838.

Ramadan T, Camargo SM, Herzog B, Bordin M, Pos KM & Verrey F (2007). Recycling of aromatic amino acids via TAT1 allows efflux of neutral amino acids via LAT2–4F2hc exchanger. *Pflugers Arch* **454**, 507–516.

Ramadan T, Camargo SM, Summa V, Hunziker P, Chesnov S, Pos KM & Verrey F (2006). Basolateral aromatic amino acid transporter TAT1 (Slc16a10) functions as an efflux pathway. *J Cell Physiol* **206**, 771–779.

Rudnick G, Krämer R, Blakely RD, Murphy DL & Verrey F (2014). The SLC6 Transporters: perspective on structure, functions, regulation and models for transporter dysfunction (2014). *Pflugers Arch* **466**, 25–42.

Shigeoka T, Kawaichi M & Ishida Y (2005). Suppression of nonsense-mediated mRNA decay permits unbiased gene trapping in mouse embryonic stem cells. *Nucleic Acids Res* **33**, e20.

Sipowicz MA, Chomarat P, Diwan BA, Anver MA, Awasthi YC, Ward JM, Rice JM, Kasprzak KS, Wild CP & Anderson LM (1997). Increased oxidative DNA damage and hepatocyte overexpression of specific cytochrome P450 isoforms in hepatitis of mice infected with *Helicobacter hepaticus. Am J Pathol* **151**, 933–941.

Soll C, Jang JH, Riener MO, Moritz W, Wild PJ, Graf R & Clavien PA (2010). Serotonin promotes tumor growth in human hepatocellular cancer. *Hepatology* **51**, 1244–1254.

Sperandeo MP, Annunziata P, Bozzato A, Piccolo P, Maiuri L, D'Armiento M, Ballabio A, Corso G, Andria G, Borsani G & Sebastio G (2007). Slc7a7 disruption causes fetal growth retardation by downregulating Igf1 in the mouse model of lysinuric protein intolerance. *Am J Physiol Cell Physiol* **293**, C191–C198.

Spoelstra MN, Mari A, Mendel M, Senga E, van Rheenen P, van Dijk TH, Reijngoud DJ, Zegers RG, Heikens GT & Bandsma RH (2012). Kwashiorkor and marasmus are both associated with impaired glucose clearance related to pancreatic beta-cell dysfunction. *Metabolism* **61**, 1224–1230.

Sterchi EE, Stocker W & Bond JS (2008). Meprins, membrane-bound and secreted astacin metalloproteinases. *Mol Aspects Med* **29**, 309–328.

Taylor MA & Smith LD (1987). Accumulation of free amino acids in growing *Xenopus laevis* oocytes. *Dev Biol* **124**, 287–290.

Verrey F, Singer D, Ramadan T, Vuille-dit-Bille RN, Mariotta L & Camargo SM (2009). Kidney amino acid transport. *Pflugers Arch* **458**, 53–60.

Wagner CA, Loffing-Cueni D, Yan Q, Schulz N, Fakitsas P, Carrel M, Wang T, Verrey F, Geibel JP, Giebisch G, Hebert SC & Loffing J (2008). Mouse model of type II Bartter's syndrome. II. Altered expression of renal sodium- and water-transporting proteins. *Am J Physiol Renal Physiol* **294**, F1373–F1380.

Wiktor-Jedrzejczak W, Bartocci A, Ferrante AW Jr, Ahmed-Ansari A, Sell KW, Pollard JW & Stanley ER (1990). Total absence of colony-stimulating factor 1 in the macrophage-deficient osteopetrotic (op/op) mouse. *Proc Natl Acad Sci U S A* **87**, 4828–4832.

Wolfsdorf JI, Sadeghi-Nejad A & Senior B (1982). Hypoalaninemia and ketotic hypoglycemia: cause or consequence? *Eur J Pediatr* **138**, 28–31.

Xie X, Dumas T, Tang L, Brennan T, Reeder T, Thomas W, Klein RD, Flores J, O'Hara BF, Heller HC & Franken P (2005). Lack of the alanine-serine-cysteine transporter 1 causes tremors, seizures, and early postnatal death in mice. *Brain Res* **1052**, 212–221.

Additional information

Competing interests

All authors declare that there are no competing financial, personal or professional interests that could be construed to have influenced this paper.

Author contributions

A.G., L.M. and F.V contributed to the conception and design of the experiment. A.G., L.M., L.B., B.H., R.F., S.M.R.C. and F.V. were involved in the collection, analysis and interpretation of data. A.G. and F.V. drafted and revised the article. All authors approved the final version submitted for publication.

Funding

The laboratory of FV is supported by Swiss NSF grant 31-130471/1 and the National Centre of Competence in Research (NCCR) Kidney.CH.

Acknowledgements

The authors thank Giancarlo Russo for his help with the analysis of the RNA sequencing data and Achim Weber for his help with the liver histological analysis.